



## Research paper

## Prognostic value of CT myocardial perfusion imaging and CT-derived fractional flow reserve for major adverse cardiac events in patients with coronary artery disease

M. van Assen<sup>a,b</sup>, C.N. De Cecco<sup>a,i</sup>, M. Eid<sup>a</sup>, P. von Knebel Doeberitz<sup>a</sup>, M. Scarabello<sup>a</sup>, F. Lavra<sup>a</sup>, M.J. Bauer<sup>a</sup>, D. Mastrodicasa<sup>a</sup>, T.M. Duguay<sup>a</sup>, B. Zaki<sup>a</sup>, G.G. Lo<sup>d</sup>, Y.H. Choe<sup>e</sup>, Y. Wang<sup>f</sup>, Pooyan Sahbaee<sup>g</sup>, Christian Tesche<sup>a,h</sup>, M. Oudkerk<sup>b</sup>, R. Vliegenthart<sup>a,b,c</sup>, U.J. Schoepf<sup>a,\*</sup>

<sup>a</sup> Division of Cardiovascular Imaging, Department of Radiology and Radiological Science, Medical University of South Carolina, Charleston, SC, USA

<sup>b</sup> University of Groningen, University Medical Center Groningen, Center for Medical Imaging - North East Netherlands, Groningen, the Netherlands

<sup>c</sup> University of Groningen, University Medical Center Groningen, Departments of Radiology, Groningen, the Netherlands

<sup>d</sup> Department of Diagnostic and Interventional Radiology, Hong Kong Sanatorium and Hospital, Happy Valley, Hong Kong, China

<sup>e</sup> Department of Radiology, Samsung Medical Center, Sungkyunkwan University School of Medicine, Seoul, Republic of Korea

<sup>f</sup> Department of Radiology, Peking Union Medical College Hospital, Chinese Academy of Medical Sciences, Beijing, China

<sup>g</sup> Siemens Medical Solutions, Malvern, PA, USA

<sup>h</sup> Department of Cardiology and Intensive Care Medicine, Heart Center Munich-Bogenhausen, Munich, Germany

<sup>i</sup> Department of Radiology, Emory University, Atlanta, Georgia, USA

## ARTICLE INFO

## Keywords:

Perfusion imaging  
Fractional flow reserve  
Coronary artery disease  
Myocardial ischemia

## STRUCTURED ABSTRACT

**Objectives:** The purpose of this study was to analyze the prognostic value of dynamic CT perfusion imaging (CTP) and CT derived fractional flow reserve (CT-FFR) for major adverse cardiac events (MACE).

**Methods:** 81 patients from 4 institutions underwent coronary computed tomography angiography (CCTA) with dynamic CTP imaging and CT-FFR analysis. Patients were followed-up at 6, 12, and 18 months after imaging. MACE were defined as cardiac death, nonfatal myocardial infarction, unstable angina requiring hospitalization, or revascularization. CT-FFR was computed for each major coronary artery using an artificial intelligence-based application. CTP studies were analyzed per vessel territory using an index myocardial blood flow, the ratio between territory and global MBF. The prognostic value of CCTA, CT-FFR, and CTP was investigated with a univariate and multivariate Cox proportional hazards regression model.

**Results:** 243 vessels in 81 patients were interrogated by CCTA with CT-FFR and 243 vessel territories (1296 segments) were evaluated with dynamic CTP imaging. Of the 81 patients, 25 (31%) experienced MACE during follow-up. In univariate analysis, a positive index-MBF resulted in the largest risk for MACE (HR 11.4) compared to CCTA (HR 2.6) and CT-FFR (HR 4.6). In multivariate analysis, including clinical factors, CCTA, CT-FFR, and index-MBF, only index-MBF significantly contributed to the risk of MACE (HR 10.1), unlike CCTA (HR 1.2) and CT-FFR (HR 2.2).

**Conclusion:** Our study provides initial evidence that dynamic CTP alone has the highest prognostic value for MACE compared to CCTA and CT-FFR individually or a combination of the three, independent of clinical risk factors.

**Abbreviations:** Arterial input function, (AIF); Coronary artery disease, (CAD); Coronary computed tomography angiography, (CCTA); CT-derived fractional flow reserve, (CT-FFR); Fractional Flow Reserve, (FFR); Interquartile range, (IQR); Major adverse cardiac events, (MACE); Myocardial blood flow, (MBF); Myocardial perfusion CT, (CTP); Standard deviation, (SD); Tissue attenuation curves, (TAC)

\* Corresponding author. Department of Radiology and Radiological Science Medical, University of South Carolina, 25 Courtenay Drive, Charleston, SC, USA.

**E-mail addresses:** [vanasse@musc.edu](mailto:vanasse@musc.edu) (M. van Assen), [carlodececco@gmail.com](mailto:carlodececco@gmail.com) (C.N. De Cecco), [p\\_knebel@hotmail.de](mailto:p_knebel@hotmail.de) (M. Eid), [p\\_knebel@hotmail.de](mailto:p_knebel@hotmail.de) (P. von Knebel Doeberitz), [marco.scarabello@gmail.com](mailto:marco.scarabello@gmail.com) (M. Scarabello), [francescolavra@libero.it](mailto:francescolavra@libero.it) (F. Lavra), [email@bauermaximilian.de](mailto:email@bauermaximilian.de) (M.J. Bauer), [domenico.mastrodicasa@gmail.com](mailto:domenico.mastrodicasa@gmail.com) (D. Mastrodicasa), [duguay@musc.edu](mailto:duguay@musc.edu) (T.M. Duguay), [zaki@musc.edu](mailto:zaki@musc.edu) (B. Zaki), [drgl@hksh.com](mailto:drgl@hksh.com) (G.G. Lo), [ychoe11@gmail.com](mailto:ychoe11@gmail.com) (Y.H. Choe), [yiningpumc@hotmail.com](mailto:yiningpumc@hotmail.com) (Y. Wang), [pooyan.sahbaee@siemens-healthineers.com](mailto:pooyan.sahbaee@siemens-healthineers.com) (P. Sahbaee), [tesche.christian@googlemail.com](mailto:tesche.christian@googlemail.com) (C. Tesche), [m.oudkerk@rug.nl](mailto:m.oudkerk@rug.nl) (M. Oudkerk), [r.vliegenthart@umcg.nl](mailto:r.vliegenthart@umcg.nl) (R. Vliegenthart), [schoepf@musc.edu](mailto:schoepf@musc.edu) (U.J. Schoepf).

<https://doi.org/10.1016/j.jcct.2019.02.005>

Received 13 December 2018; Accepted 11 February 2019

Available online 12 February 2019

1934-5925/ Published by Elsevier Inc. on behalf of Society of Cardiovascular Computed Tomography

## 1. Introduction

Coronary computed tomography angiography (CCTA) has become an established, widely accepted imaging technique to evaluate coronary artery disease (CAD). However, CCTA provides only anatomic information and is a poor predictor of the functional significance of a stenosis with a tendency to overestimate stenosis severity.<sup>1–4</sup> Over the past decade, functional parameters have become more important for patient management.<sup>5</sup>

Non-invasive Fractional Flow Reserve (FFR) derived from CCTA (CT-FFR) provides incremental diagnostic value over CCTA alone by adding functional information.<sup>6–11</sup> Among the advantages of CT-FFR is the fact that no additional acquisition is needed and no stressor agent is used, as is often the case with other non-invasive functional evaluation techniques.<sup>12</sup> Several studies show high discriminatory accuracy of CT-FFR to detect hemodynamically significant stenosis compared to invasive FFR.<sup>6,7,13–15</sup>

Dynamic myocardial perfusion CT (CTP) imaging performed during pharmacologic stress has been described as complementary to CCTA for assessing the functional significance of coronary artery stenoses.<sup>8</sup> The unique advantage of dynamic myocardial CTP imaging is the possibility of absolute quantification of myocardial blood flow (MBF) and the ability to assess anatomical and functional parameters of a coronary artery stenosis using a single modality. The added value of dynamic CTP over CT-FFR is the fact that CTP analyzes the directly the myocardial bloodflow. Multiple studies show excellent accuracy of CTP in assessing the functional significance of a stenosis.<sup>16–21</sup>

Only a few studies have investigated the prognostic value of CT-FFR and dynamic CTP.<sup>17,22,23</sup> A study on the prognostic value of CT-FFR for major adverse cardiac events (MACE) showed that patients with a pathologic CT-FFR value had a 4.3-fold higher risk of MACE than patients with normal CT-FFR, using a CT-FFR cut-off of 0.80.<sup>23</sup> Studies on dynamic CTP imaging show that patients with visually detected perfusion defects are up to 4.8 times more likely to suffer a MACE, depending on the number of territories involved.<sup>17</sup>

The purpose of this study was to intra-individually analyze and compare the prognostic value of dynamic CTP and CT-FFR in predicting MACE.

## 2. Methods

### 2.1. Population

The population for this study was enrolled in a global multicenter registry with 4 participating centers in Asia, Europe, and the US. Portions of this study population have been previously reported.<sup>24–26</sup> In this population CT perfusion was performed for research purposes. However, CT-FFR analysis was not performed and the prognostic value of CT-FFR in combination with CCTA and dynamic CTP on future MACE was not assessed in these studies.

Patients were included in the original study if they had suspected or known CAD. Patients were excluded if they had contraindications to CT, iodinated contrast medium, or adenosine. The following demographic parameters and baseline clinical risk factors were recorded for all included patients: age, sex, history of diabetes/hypertension/dyslipidemia, smoking history, history of CAD, and family history of CAD. The respective research study protocols had been approved by the institutional review boards of all participating institutions, and written informed consent had been obtained from all research subjects before enrollment.

From this multicenter registry, we selected data from patients who had undergone CCTA and dynamic myocardial CTP imaging and had a follow up period of 18 months or until MACE occurred. Patients with stents, bypasses, incomplete follow-up data, or poor image quality of either the CCTA or the dynamic CTP study were excluded. Patients with a history of CAD, such as known MI or ischemia, without intervention

were not excluded from analysis.

### 2.2. Imaging protocols

All image acquisitions were performed with a second-generation dual-source CT system (SOMATOM Definition Flash, Siemens Healthineers, Forchheim, Germany). CCTA was performed after administering 50–80 mL of iodinated contrast material with a concentration of 300–370 mg I/mL at a flow rate of 4–5 mL/s. Depending on heart rate and rhythm, the CCTA acquisition was performed with retrospective ECG gating in case of arrhythmias, prospectively ECG-triggered sequential acquisition in case of regular heart rates above 60 beats/min, or prospectively ECG triggered high-pitch spiral acquisition in case of regular heart rates under 60 beats/min. After 3–4 min of adenosine administration (140 µg/kg/min), the dynamic CTP acquisition was initiated. Data acquisition was performed for 30 s with both x-ray tubes at 100 kV, gantry rotation time of 0.28 s, and tube current of 300 mAs per rotation. CTP imaging was performed with an ECG-triggered shuttle mode (two alternating table positions) with a systolic image acquisition (250 ms after the R wave). The perfusion images were acquired after the administration of 40–50 mL of iodinated contrast agent with a concentration of 300–370 mg I/mL, administered at a flow rate of 4–7.5 mL/s.

### 2.3. Image analysis

All CCTA and CTP studies were assessed for image quality on a 4-point Likert scale (1- poor image quality, 4 excellent image quality). Patients with poor image quality were excluded from analysis.

#### 2.3.1. CCTA evaluation

CCTA datasets were reconstructed with a section thickness of 0.75 mm and 0.5 mm increments with a vascular reconstruction kernel (B26F). Two experienced readers (3 and 6 years of experience in cardiac CT interpretation) independently evaluated all CCTA studies. The presence of stenosis was assessed in the left anterior descending, left circumflex, and right coronary artery. The left main coronary artery was included with the left anterior descending. The degree of stenosis was assessed with multiplanar reformats and curved multiplanar reconstructions along the vessel centerline (Circulation, Siemens). Vessels were visually assessed as to whether they had no stenosis, stenosis < 50% or stenosis ≥ 50%. A CCTA was considered positive if there was a stenosis ≥ 50% in any vessel. Additionally, coronary artery dominance (right, left, or co-dominance) was recorded.

#### 2.3.2. CT-FFR evaluation

CT-FFR was computed using an on-site prototype application (cFFR version 3.0, Siemens, not currently commercially available), which has been previously described.<sup>7,15,27</sup> With this software a three-dimensional coronary model was semi-automatically segmented, after which markers were manually placed proximal and distal to each stenotic lesion. CT-FFR values were recorded for each vessel, distal to any stenotic lesions, when present. In case of multiple stenoses, the CT-FFR value distal to the most severe lesion was used. In case of no stenosis, the CT-FFR value from the mid-segment of the vessel was recorded. For the prognostic analysis, the lowest FFR-value of each patient was used. A CT-FFR value above the optimal cut-off threshold, as described in the statistical analysis section, was considered negative.

#### 2.3.3. Dynamic CT perfusion evaluation

CTP studies were analyzed using a dedicated software package (Volume Perfusion CT body, Siemens). Motion correction was applied to all images. MBF was calculated using tissue attenuation curves (TAC) and the arterial input function (AIF) with a hybrid deconvolution method. The AIF was sampled in the descending aorta. By using images from both table positions, a double sampled AIF was generated to

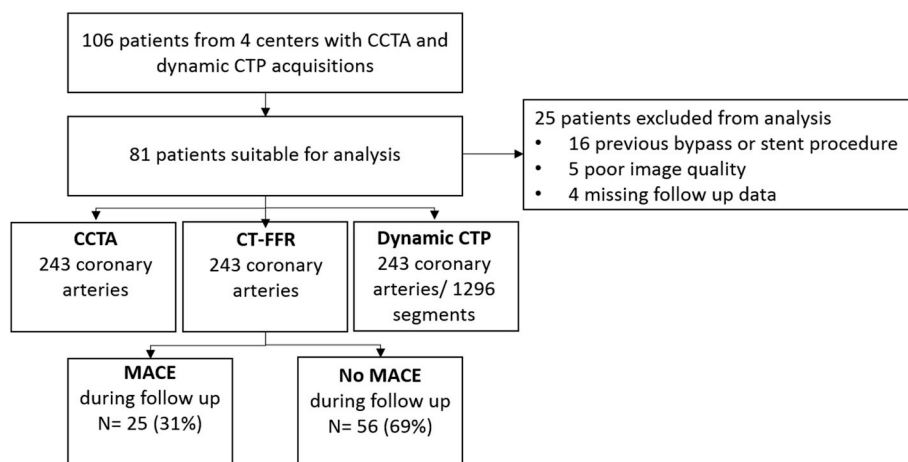


Fig. 1. Flowchart patient selection. MACE, major adverse cardiac events.

increase accuracy. MBF maps were reconstructed as color-coded images (section thickness 3.0 mm, increment 1.5 mm). MBF was evaluated on a per segment basis, according to the 17-segment AHA myocardial model, with exclusion of the apical (17th) segment. After the segmentation, each segment was attributed to a vessel territory, taking into account the coronary artery dominance. An index-MBF was calculated to account for inter-patient differences in MBF. The index-MBF was calculated as a ratio between territory and global MBF. For our analysis, the lowest index-MBF out of the three territories was used. An index-MBF above the optimal cut-off threshold, as described in the statistical analysis section, was considered negative.

#### 2.4. Clinical follow-up

All study subjects underwent prospective follow-up by chart review and telephone interviews with the patient or an immediate relative at 6, 12, and 18 months after imaging. Reported clinical events were confirmed by contact with the patient's primary care physician or the admitting hospital. At each time point, the occurrence of MACE was recorded. MACE were defined as cardiac death, non-fatal myocardial infarction, unstable angina requiring hospitalization, or revascularization (percutaneous coronary intervention or coronary artery bypass grafting) and used as the primary end-point of this study. Hard MACE was defined as MACE excluding revascularizations. CT-FFR and CTP images were retrospectively analyzed at a central location and findings from these acquisitions had no influence on the diagnostic work-up and were not used for treatment management. Patients who underwent revascularizations that followed directly from the CCTA images were excluded from our initial population.

#### 2.5. Statistical analysis

Continuous variables are represented as mean (standard deviation [SD]) or median (interquartile range [IQR]), depending on their distribution (tested with Shapiro Wilks test). Categorical data is displayed as absolute frequencies and proportions. The difference between the MACE positive and MACE negative patients was evaluated with an unpaired, 2-sided Mann-Whitney *U* test. The CT-FFR and index-MBF values for MACE negative and MACE positive cases were compared using an unpaired, 2-sided Mann-Whitney *U* test. A Chi-square test was used to compare the frequency distribution of categorical and binary data between groups. Optimal thresholds for CT-FFR and index-MBF values to predict MACE were calculated using the Youden index. A grey zone of CT-FFR values between 0.70 and 0.80 was determined by the range of FFR cut-off thresholds, currently used in clinical (invasive FFR) and research (CT-FFR) contexts. The univariate Cox proportional

hazards regression model was used to analyze the prognostic value of findings at CCTA, CT-FFR and index-MBF individually for MACE during follow-up. Multivariate Cox proportional hazards regression analysis was performed to evaluate whether the prognostic value of each parameter was independent of the other imaging parameters and whether they were independent of age, sex, and clinical risk factors, including hypertension, hyperlipidemia, diabetes, smoking history, and family history of CAD. Using multivariate analysis, a combination of CCTA and CT-FFR, CCTA and index-MBF and CCTA, CT-FFR and index-MBF was investigated, with or without correction for clinical data. Statistical analyses were conducted using SPSS version 23 (IBM, Armonk, New York). MedCalc version 13.0 (MedCalc Software, Ostend, Belgium) was used to compare the areas under the curve (AUCs) using the method of DeLong et al.

### 3. Results

From the initial population of 106 patients with CCTA and dynamic CT perfusion imaging, 16 were excluded because of previously implanted stents and coronary artery bypass grafts, 5 were excluded because of poor image quality, and 4 were excluded because of incomplete follow up, see Fig. 1. The final study population consisted of 81 patients, in whom 243 vessels were investigated on CCTA with CT-FFR and 243 vessel territories (1296 segments) were evaluated with dynamic CTP. The mean follow-up period was 15.7 months (SD 4.7). Of these 81 patients, 25 (31%) experienced MACE in their follow up period. Of the MACE positive patients, 11 patients (14%) experienced a hard MACE, including unstable angina, myocardial infarction, or cardiac death, 14 (17%) patients were considered MACE positive because of revascularizations. Table 1 gives an overview of the patient demographics.

#### 3.1. CCTA

Of the total 243 vessels analyzed on CCTA, 104 had no stenotic lesions, 92 had a lesion with < 50% stenosis, and 47 had a stenosis  $\geq$  50%. An overview of the CCTA findings for all patients, MACE positive and MACE negative patients is provided in Table 2. In the MACE positive group, 14 (56%) patients had a stenosis  $\geq$  50% in any of the vessels according to CCTA, in the MACE negative group, 14 (25%) patients had a CCTA-derived stenosis  $\geq$  50%.

#### 3.2. CT-FFR

An overview of the CT-FFR findings for all patients, MACE positive and MACE negative patients is provided in Table 2. The MACE positive

**Table 1**  
Patient characteristics.

	Total	MACE -	MACE +	p-value
	N = 81	N = 56 (69)	N = 25 (31)	
Age, yrs	60.2 (9.8)	60.5 (10.0)	59.5 (9.6)	0.677
Male	59 (72.8)	39 (69.8)	20 (80.0)	0.423
<b>Cardiovascular risk factors</b>				
Hypertension	39 (48.1)	29 (51.8)	10 (40.0)	0.612
Dyslipidemia	36 (44.4)	27 (48.2)	9 (36.0)	0.458
Diabetes	22 (27.2)	14 (25)	8 (32.0)	0.414
Family history of CAD	18 (22.2)	13 (23.2)	5 (20.0)	1.000
History of smoking	25 (30.9)	19 (33.9)	6 (24.0)	0.594
<b>Right Dominance</b>	74 (91.4)	49 (87.5)	25 (100)	0.181
<b>Revascularizations</b>	N = 14			
PCI	13 (16)			
CABG	1 (1)			
<b>MACE</b>	N = 11			
Death	1 (1)			
Non-fatal myocardial infarction	3 (4)			
Unstable agina	7 (9)			

Values are given as mean  $\pm$  SD, n (%). A p-value < 0.05 is considered significant. CAD: coronary artery disease.

**Table 2**  
Overview CCTA, CT-FFR and index MBF results.

	CCTA	CT-FFR	Index-MBF
<b>Overall patients (n = 243)</b>	Significant lesions		
LAD	23 (28)	0.87 (0.74–0.94)	1.00 (0.91–1.13)
RCA	13 (16)	0.92 (0.81–0.96)	1.08 (0.98–1.17)
Cx	11 (14)	0.89 (0.81–0.94)	1.00 (0.84–1.07)
<b>MACE Negative patients (n = 56)</b>			
Parameter value overall	–	0.84 (0.75–0.90)	0.95 (0.87–1.00)
Negative test n(%)	42 (75)	45 (80)	42 (75)
Parameter value	–	0.87 (0.80–0.94)	0.98 (0.93–1.03)
Positive test n(%)	14 (25)	11 (20)	14 (25)
Parameter value	–	0.58 (0.37–0.66)	0.63 (0.52–0.79)
1 vessel/territory	2 (14)	5 (45)	10 (71)
2 vessel/territory	8 (57)	5 (45)	4 (29)
3 vessel/territory	4 (29)	1 (10)	0 (0)
<b>MACE Positive patients (n = 25)</b>			
Parameter value overall	–	0.71 (0.64–0.84)	0.72 (0.57–0.85)
Negative test n(%)	11 (44)	9 (36)	3 (12)
Parameter value	–	0.87 (0.80–0.89)	0.99 (0.96–0.99)
Positive test n(%)	14 (56)	16 (64)	22 (88)
Parameter value	–	0.67 (0.50–0.71)	0.67 (0.52–0.78)
1 vessel/territory	11 (79)	11 (69)	16 (73)
2 vessel/territory	3 (21)	4 (25)	5 (23)
3 vessel/territory	0 (0)	1 (6)	1 (4)

Values are given as mean  $\pm$  SD, n (%). LAD: left anterior descending coronary artery, RCA: right coronary artery, Cx: circumflex coronary artery.

group had 9 patients with non-pathological CT-FFR values, and 16 patients with CT-FFR values indicating lesion specific ischemia. The MACE negative group had 45 (80%) patients with CT-FFR values > 0.80 and 11 (20%) patients with positive CT-FFR values. The median CT-FFR values for MACE positive patients was 0.71 (IQR: 0.64 to 0.84), which was significantly lower than the median CT-FFR value in MACE negative patients, 0.84 (IQR: 0.75 to 0.90, p-value = 0.004). The optimal threshold computed using the Youden index was a CT-FFR value of 0.75.

### 3.3. Dynamic CT perfusion

The index MBF findings for all patients, MACE positive, and MACE negative patients are summarized in Table 2. Global MBF was similar in

the MACE negative (median 130.0 mL/100 mL/min; IQR: 112.5–146.3) and MACE positive (median 138.0; IQR 109.0–151.0) patients. The MACE positive group had 3 (12%) patients without positive index-MBF, and 22 (88%) patients with a positive index-MBF. The three MACE positive patients with a negative index-MBF all had revascularizations and no hard MACE. The MACE negative group had 42 (75%) patients without a positive index-MBF and 14 (25%) patients with a positive index MBF. The median lowest index MBF values for MACE positive patients was 0.72 (IQR: 0.57 to 0.85), which was significantly lower than the median index MBF value in MACE negative patients, 0.95 (IQR: 0.87 to 1.00), p-value < 0.001. The optimal threshold for the index MBF was 0.88, as computed by the Youden index.

### 3.4. CT-FFR and dynamic CT perfusion

Correct classification of MACE was reached by both CT-FFR and index MBF in 60 patients (74%). In cases of disagreement between CTP and CT-FFR (21 patients), CTP predicted MACE correctly in 12 patients (57%), and in 8 (38%) cases CT-FFR predicted MACE correctly. Fig. 2 shows a case in which CT-FFR and index-MBF are in agreement and a case in which CT-FFR and index-MBF were discordant. Especially in cases of negative CTP and positive CT-FFR, CTP was most predictive of outcome (83% of patients correctly classified), see Fig. 3. Interestingly, in the patients with discordant imaging tests, the median CT-FFR value in MACE negative patients (0.75; 0.63–0.87 (n = 13)) was lower than the CT-FFR value in MACE positive patients (0.84; 0.71–0.88 (n = 8)). The index MBF values were lower in the MACE negative group (0.72; 0.63–0.91) than in the MACE positive group (0.81; 0.69–0.86) for patients with discordant tests. However, differences in both CT-FFR and index-MBF were not statistically significant (p-value of 0.972 and 0.301).

The grey zone for CT-FFR was determined to be between 0.70 and 0.80, including the clinically used range for FFR cut-off thresholds. In the group of patients with CT-FFR values in the grey zone, the MACE positive patients (n = 8) had a significantly lower index MBF (0.69, IQR: 0.56 to 0.73) than the MACE negative group (0.97, IQR: 0.81 to 1.02, p-value = 0.007). All 8 MACE positive patients had a positive index-MBF and of the MACE negative patients, 3 (25%) had a positive index-MBF. Of the MACE positive patients with a grey zone CT-FFR value, 50% received revascularization.

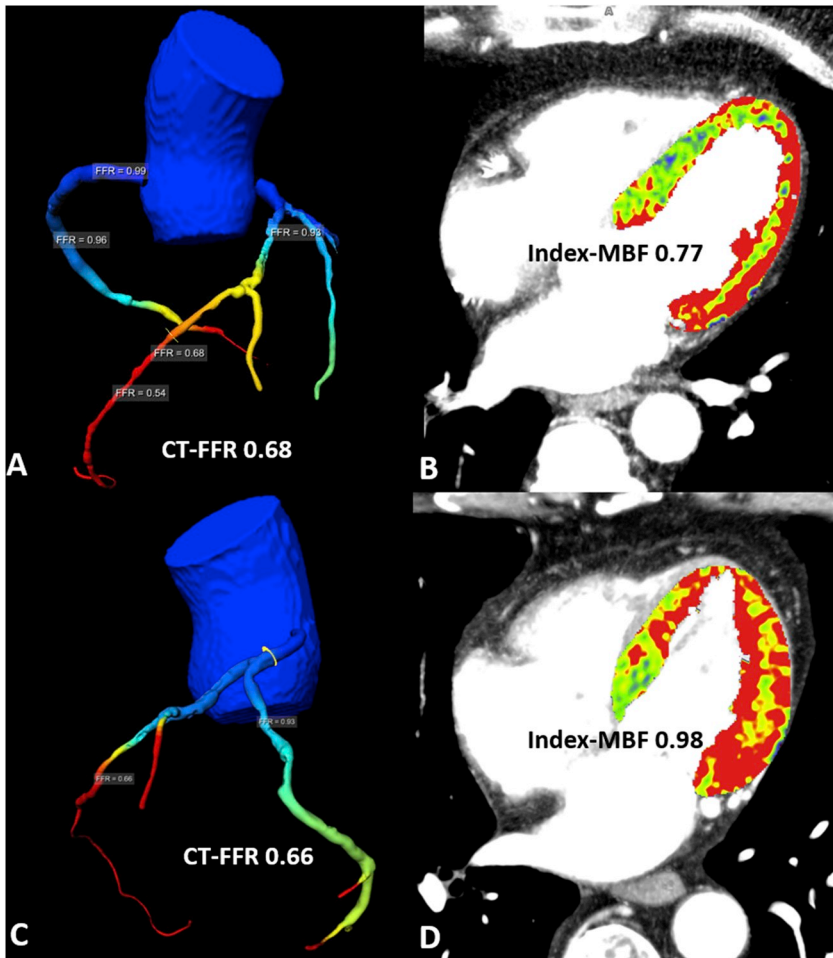
### 3.5. Prognostic value of imaging findings

Table 3 shows an overview of the results of the Cox proportional hazards regression models. Patients with at least one > 50% stenosis on CCTA images were significantly more likely to experience MACE during follow-up (HR 2.7 (95% CI 1.2–5.9); p-value 0.0015). This effect was independent of clinical information (age, gender, and risk factors), however it lost significance when CT-FFR, index MBF, or both were taken into consideration. Patients with a positive CT-FFR value (i.e., < 0.75) in at least one coronary artery were at significantly increased risk of MACE (HR 4.6 (95% CI 2.0–10.5); p-value < 0.001). This association remained significant after adjustment for age, sex, and clinical risk factors and when CCTA findings were considered (HR 3.7(95% CI 1.2–11.1); p-value 0.019). When index-MBF was taken into account, CT-FFR lost its significance (HR 2.2 (95% CI 0.8–6.4); p-value 0.130).

Patients with a perfusion defect in at least one vascular territory according to index-MBF (< 0.88) were at increased risk of MACE (HR 11.4 (95% CI 3.4–38.2); p-value < 0.001). This association remained statistically significant after adjusting for CCTA, CT-FFR findings, age, sex, and clinical risk factors (HR 10.1 (95% CI 2.1–48.8) p-value 0.004).

## 4. Discussion

The present study evaluated the prognostic value of CCTA, CT-FFR,



**Fig. 2.** Panels A and B represent a MACE positive patient, (age 63, male). The CT-FFR illustration (A) shows a hemodynamically significant LAD lesion with a FFR-value of 0.68 that decreases to 0.54 distally (CT-FFR < 0.75 is considered positive). On the dynamic CTP (B) a perfusion defect is shown (black arrow), classified as ischemic with an index-MBF of 0.77 (index-MBF < 0.88 is considered positive). Panels C and D represent a MACE negative patient (age 52, male). The second CT-FFR illustration (C) shows a hemodynamically significant lesion in the LAD with a FFR-value of 0.66, without a corresponding positive index-MBF value (D) (0.98). CT-FFR; CT derived fractional flow reserve, Index-MBF, myocardial blood flow ratio between territory and global flow.

and dynamic CTP imaging for MACE. Our results demonstrate that index-MBF calculated from dynamic CTP acquisitions has the highest prognostic value, over CCTA and CT-FFR values, or a combination of the three. In univariate analysis, the presence of a positive index-MBF resulted in the largest risk for MACE (HR 11.4) compared to CCTA (HR 2.6) and CT-FFR (HR 4.6). In multivariate analysis, only index-MBF significantly contributed to the risk of MACE (HR 10.1), unlike CCTA (HR 1.2) and CT-FFR (HR 2.2).

The strong prognostic value of myocardial perfusion evaluation is in line with evidence from a large number of nuclear perfusion studies, showing that the presence and extent of perfusion defects found with SPECT and PET are highly predictive of MACE with HRs ranging from 2.3 to 6.45.<sup>28–34</sup> The HRs found in this study are higher, which could be caused by the capability of CT perfusion to absolutely quantify MBF and by the high-risk population investigated in this study.

In our opinion, this observation is also in accordance with the fact that CT-FFR is an indirect measure of myocardial ischemia induced by atherosclerotic lesions, whereas dynamic CTP provides a direct quantitative assessment of myocardial perfusion. A positive CT-FFR result does not directly translate in myocardial ischemia. This is especially true when CT-FFR values fall in the grey area, where the accuracy significantly decreases (from 70–86% to 55–68% in the grey zone).<sup>6,8</sup> The grey zone is also seen with invasive FFR, where myocardial perfusion imaging confirmed that a FFR value of  $\leq 0.75$  results in stress-inducible myocardial ischemia. Other studies demonstrated that revascularization of coronary stenosis with a FFR > 0.75 did not improve clinical outcomes whereas using FFR  $\leq 0.80$  did.<sup>35–37</sup> Moreover, by measuring the myocardial blood flow directly, dynamic CTP does not only detect stenotic specific ischemia but can also detect

microcirculatory impairment.<sup>38</sup> Coronary microcirculatory dysfunction may be an early indicator of CAD and is associated with a wide range of myocardial diseases and can affect patient outcomes.<sup>39,40</sup> The CT-FFR measurement predominantly interrogates conditions in the main coronary arteries and larger branches, but fails to reflect the effect of microvascular disease or collateral vessels, thus providing an indirect and partial overview of the status of the myocardium. Furthermore, the location of the CT-FFR measurement could influence the correlation with dynamic CTP measurements - a distal flow-obstructive CT-FFR measurements is expected to have a smaller effect on myocardial blood flow than a proximal pathological CT-FFR value. The added value of CTP in the CT-FFR grey area is supported by our sub-analysis where we demonstrated that CTP was effective in predicting MACE, with the positive patients having a significantly lower index MBF than the MACE negative group. This finding is also confirmed by a recent study demonstrating the incremental diagnostic role of myocardial perfusion assessment in the grey zone with an increase in accuracy from 55% using only CT-FFR to 77% with the addition of dynamic CTP image analysis.<sup>8</sup>

Previous studies comparing invasive FFR and PET derived flow demonstrated only a moderate correlation, with reported  $r^2$  values of 0.15 and  $r$  values of 0.34–0.36.<sup>41,42</sup> Although there is correlation between the hemodynamically significance of a stenosis measured with FFR and blood flow, it is not a direct relationship and many factors can influence this correlation, which in turn can influence the relationship to outcomes.<sup>41–43</sup>

Moreover, CT-FFR demonstrates superiority to stenosis severity on CCTA for MACE prognostication (HR 4.6 for CT-FFR vs. 2.7 for CCTA). This reflects the high sensitivity and negative predictive value of CCTA,

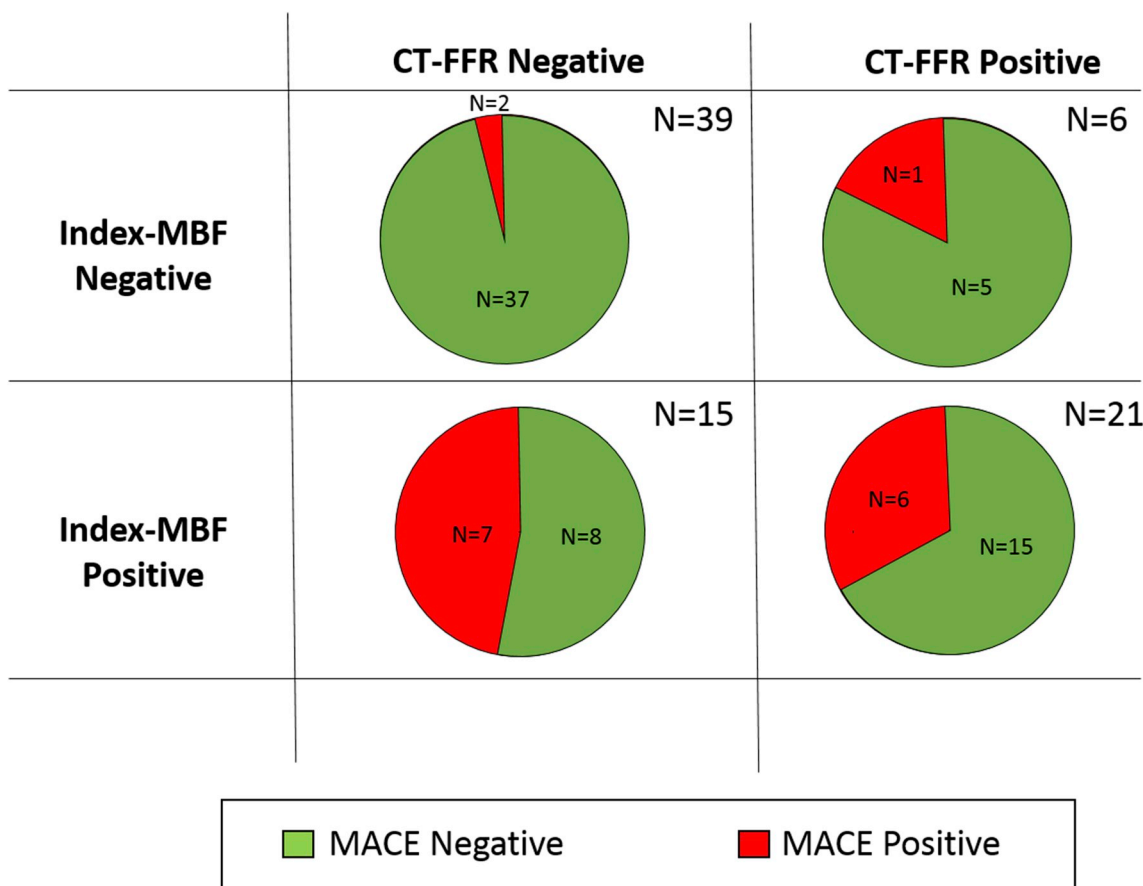


**Fig. 3.** Classification by CT-FFR and index-MBF. Correct classification was reached by both CT-FFR and index-MBF in 60 patients (74%). In cases of disagreement between index-MBF and CT-FFR (21 patients), index-MBF predicted MACE correctly in 12 patients (57%). In patients with a negative CTP and a positive CT-FFR, index-MBF was most predictive of outcome (83% of patients). CT-FFR; CT derived fractional flow reserve, Index-MBF, myocardial blood flow ratio between territory and global flow.

along with the incremental value of CT-FFR owed to the increased specificity for the detection of flow-limiting stenosis, especially in the cases of intermediate stenosis.<sup>44</sup>

A similar study on the prognostic value of CT-FFR for MACE showed that patients with a positive CT-FFR value ( $\leq 0.80$ ) had 4.3-fold higher risk of MACE than patients with a negative CT-FFR value ( $> 0.80$ ).<sup>23</sup> Our study shows a similar HR of 4.6 for at least one positive vessel with

CT-FFR  $< 0.75$ . Of note, the CT-FFR cut-off threshold used in our study differs from other CT-FFR studies where a value of 0.80 was applied for detecting functionally significant stenosis.<sup>23</sup> However, in those studies the cut-off was determined for stenosis detection, whereas our threshold was derived from MACE. Moreover, the threshold determined in this study still falls within the range of thresholds (0.75–0.80) used in other studies investigating the prognostic value of invasive FFR.<sup>45–47</sup> A

**Table 3**  
Risk of major adverse cardiac events associated.

Modality	Prognostic value						
	Imaging Only			Corrected for Clinical data			
	Hazard Ratio	95% confidence interval	P-value	Hazard Ratio	95%confidence interval	P-value	
CCTA	2.7	(1.2–5.9)	0.015	4.6	(1.8–11.7)	0.002	
CT-FFR	4.6	(2.0–10.5)	$< 0.001$	5.0	(2.1–14.1)	$< 0.001$	
Index-MBF	11.4	(3.4–38.2)	$< 0.001$	14.9	(3.4–64.6)	$< 0.001$	
CCTA and CT-FFR	CCTA	1.4	(0.6–3.4)	0.459	2.3	(0.8–6.8)	0.122
	CT-FFR	3.9	(1.5–9.9)	0.004	3.7	(1.2–11.1)	0.019
CCTA and index-MBF	CCTA	1.2	(0.5–2.8)	0.636	1.7	(0.6–4.5)	0.321
	Index MBF	10.5	(3.0–36.9)	$< 0.001$	11.9	(2.6–55.7)	0.002
CCTA and CT-FFR and index-MBF	CCTA	0.9	(0.4–2.1)	0.801	1.2	(0.4–3.5)	0.758
	CT-FFR	2.3	(0.9–5.9)	0.080	2.2	(0.8–6.4)	0.130
	Index MBF	8.5	(2.3–30.9)	0.001	10.1	(2.1–48.8)	0.004

Hazard Ratio with MACE as outcome for CCTA, CT-FFR, index MBF, and combined (CCTA and CTA FFR, CCTA and index MBF; CCTA, CT-FFR, and index MBF) analyses. The first analysis takes only imaging data into account, the second model corrects for age, gender and number of risk factors.

CT computed tomography; CCTA coronary computed tomography angiography; FFR fractional flow reserve; MBF myocardial blood flow; TP true positive; FP false positive; TN true negative; FN false negative.

recent meta-analysis on the prognostic value of invasive FFR further shows that the optimal threshold for predicting death, MI, and revascularizations was 0.76, which is similar to the CT-FFR threshold determined in the current study.<sup>45</sup>

A previous investigation on a subset of patients from the same multicenter registry used in this study including 144 patients showed a HR between 2.03 and 2.50 for MACE based on visual analysis of dynamic CTP studies.<sup>17</sup> Our study shows HRs between 8.5 and 14.9 for index MBF. Although these results are based on patient populations from the same registry, they show very different HRs. This could be attributed to the additional exclusion criteria required for the CT-FFR analysis and the corresponding smaller population. Another reason causing the difference could be the difference in analysis, with the actual study focused on the quantitative analysis of the dynamic CTP acquisition instead of visual analysis. Studies on quantitative analysis of perfusion data show that quantitative analysis can detect perfusion deficits that seem visually homogenous<sup>28,29,38</sup> and add to the prognostic value of myocardial perfusion imaging.

Several limitations of this investigation have to be discussed. The population investigated in this study showed a very high disease burden, corresponding with the high number of MACE (31%) compared to previous studies on cardiac imaging and MACE.<sup>22</sup> This is most likely caused by our study design and selection criteria. Whether the investigated techniques and the combinational approach will show similar results in a population at lower risk has to be further investigated. Due to extensive inclusion and exclusion criteria, only a moderate number of patients were included in the analysis. This resulted in wide confidence intervals in the HR calculation. A larger population is needed to confirm our results and to investigate the influence of the number of territories involved in both CT-FFR and dynamic CTP. Previous studies on the predictive value of dynamic CTP showed that the number of territories with perfusion defects or the amount of myocardium involved was strongly predictive of MACE.<sup>22,48</sup> Taking the number of positive territories into account could increase the prognostic value of index MBF. With CT-FFR the same issue occurs - this study only took into account whether one vessel had a positive CT-FFR value. The number of vessels involved and the location of the stenosis could improve the prognostic value of CT-FFR. Several studies on dynamic CTP have shown that relative measurements of MBF rather than absolute MBF values are more suitable to diagnose significant CAD.<sup>25,26,49</sup> With this investigation the MBF was indexed using the average MBF of the entire myocardium of the left ventricle. However, results show a minimal effect of using an index MBF on false negative predictions, with a very low prevalence of three vessel disease ( $n = 1$ ) in this group. Finally, all examinations were acquired using a dual-source CT system of a single vendor. The CT-FFR software used in this study is a prototype from that vendor and is currently not clinically available. Generalization of our results to CT systems and software from other vendors remains unclear and needs further investigation.

In conclusion, our study provides initial evidence that in a population with suspected or known CAD, dynamic CTP has the highest predictive value for MACE compared to CCTA and CT-FFR, (individually and in combination of the three), independent of clinical factors, adding evidence to the role of CT myocardial perfusion imaging as a strong predictor of clinical outcome.

## Disclosures

Dr. Schoepf receives institutional research support from Astellas, Bayer, and Siemens. Dr. De Cecco receives institutional research support from Siemens. Dr. Schoepf has received consulting fees and or speaker honoraria from Bayer, GE, Guerbet, HeartFlow Inc., and Siemens. Dr. De Cecco has received speaker honoraria from Bayer. UMCG receives institutional research support from Siemens. The other authors have no conflict of interest to disclose.

## Appendix A. Supplementary data

Supplementary data to this article can be found online at <https://doi.org/10.1016/j.jcct.2019.02.005>.

## References

- Miller JM, Rochitte CE, Dewey M, et al. Diagnostic performance of coronary angiography by 64-row CT. *N Engl J Med*. 2008;359(22):2324–2336. <https://doi.org/10.1056/NEJMoa0806576>.
- Meijboom WB, Meijjs MFL, Schuijff JD, et al. Diagnostic accuracy of 64-slice computed tomography coronary angiography. A prospective, multicenter, multivendor study. *J Am Coll Cardiol*. 2008;52(25):2135–2144. <https://doi.org/10.1016/j.jacc.2008.08.058>.
- Meijboom WB, Van Mieghem CAG, van Pelt N, et al. Comprehensive assessment of coronary artery stenoses. Computed tomography coronary angiography versus conventional coronary angiography and correlation with fractional flow reserve in patients with stable Angina. *J Am Coll Cardiol*. 2008;52(8):636–643. <https://doi.org/10.1016/j.jacc.2008.05.024>.
- Maroules CD, Rajiah P, Bhasin M, Abbara S. Growing evidence for coronary computed tomography angiography as a first-line test in stable chest pain. *J Thorac Imag*. 2018;00(00):1. <https://doi.org/10.1097/RTI.0000000000000357>.
- Vliegenthart R, Henzler T, Moscariello A, et al. CT of coronary heart disease: Part 1, CT of myocardial infarction, ischemia, and viability. *Am J Roentgenol*. 2012;198(3):531–547. <https://doi.org/10.2214/AJR.11.7082>.
- Kruk M, L Wardziak, Demkow M, et al. Workstation-based calculation of CTA-based FFR for intermediate stenosis. *JACC Cardiovasc Imaging*. 2016;9(6):690–699. <https://doi.org/10.1016/j.jcmg.2015.09.019>.
- Coenen A, Lubbers MM, Kurata A, et al. Fractional flow reserve computed from noninvasive CT angiography data: diagnostic performance of an on-site clinician-operated computational fluid dynamics algorithm. *Radiology*. 2015;274(3):674–683. <https://doi.org/10.1148/radiol.14140992>.
- Coenen A, Rossi A, Lubbers MM, et al. Integrating CT Myocardial Perfusion and CT-FFR in the Work-Up of Coronary Artery Disease. *JACC Cardiovasc Imaging*; 2016 <https://doi.org/10.1016/j.jcmg.2016.09.028> 2014.
- Leipsic J, Yang TH, Thompson A, et al. CT Angiography (CTA) and diagnostic performance of noninvasive fractional flow reserve: results from the determination of fractional flow reserve by anatomic CTA (DeFACTO) study. *Am J Roentgenol*. 2014;202(5):989–994. <https://doi.org/10.2214/AJR.13.11441>.
- Kitabata H, Leipsic J, Patel MR, et al. Incidence and predictors of lesion-specific ischemia by FFRCT: learnings from the international ADVANCE registry. *J Cardiovasc Comput Tomogr*. 2018;12(2):95–100. <https://doi.org/10.1016/j.jcct.2018.01.008>.
- Schwartz FR, Koweek LM, Nørgaard BL. Current evidence in cardiothoracic imaging. *J Thorac Imag*. 2018;00(00):1. <https://doi.org/10.1097/RTI.0000000000000369>.
- Benton SMJ, Tesche C, De Cecco CN, Duguay TM, Schoepf UJ, Bayer RRII. Noninvasive derivation of fractional flow reserve from coronary computed tomographic angiography: a review. *J Thorac Imag*. 2018;33(2) [https://journals.lww.com/thoracimaging/Fulltext/2018/03000/Noninvasive\\_Derivation\\_of\\_Fractional\\_Flow\\_Reserve.4.aspx](https://journals.lww.com/thoracimaging/Fulltext/2018/03000/Noninvasive_Derivation_of_Fractional_Flow_Reserve.4.aspx).
- Baumann S, Wang R, Schoepf UJ, et al. Coronary CT angiography-derived fractional flow reserve correlated with invasive fractional flow reserve measurements – initial experience with a novel physician-driven algorithm. *Eur Radiol*. 2015;25(4):1201–1207. <https://doi.org/10.1007/s00330-014-3482-5>.
- Min JK, Leipsic J, Pencina MJ, et al. Diagnostic accuracy of fractional flow reserve from anatomic CT angiography. *Jama*. 2012;308(12):1237. <https://doi.org/10.1001/2012.jama.11274>.
- Renker M, Schoepf UJ, Wang R, et al. Comparison of diagnostic value of a novel noninvasive coronary computed tomography angiography method versus standard coronary angiography for assessing fractional flow reserve. *Am J Cardiol*. 2014;114(9):1303–1308. <https://doi.org/10.1016/j.amjcard.2014.07.064>.
- Wang Y, Qin L, Shi X, et al. Adenosine-stress dynamic myocardial perfusion imaging with second-generation dual-source CT: comparison with conventional catheter coronary angiography and SPECT nuclear myocardial perfusion imaging. *Am J Roentgenol*. 2012;198(3):521–529. <https://doi.org/10.2214/AJR.11.7830>.
- Meinel FG, Pugliese F, Schoepf UJ, et al. Prognostic value of stress dynamic myocardial perfusion CT in a multicenter population with known or suspected coronary artery disease. *Am J Roentgenol*. 2017;208(4):761–769. <https://doi.org/10.2214/AJR.16.16186>.
- Varga-Szemes A, Meinel FG, De Cecco CN, et al. CT myocardial perfusion imaging. *AJR Am J Roentgenol*. 2015;204(3):487–497. <https://doi.org/10.2214/AJR.14.13546>.
- Bamberg F, Marcus RP, Becker A, et al. Dynamic myocardial CT perfusion imaging for evaluation of myocardial ischemia as determined by MR imaging. *JACC Cardiovasc Imaging*. 2014;7(3):267–277. <https://doi.org/10.1016/j.jcmg.2013.06.008>.
- Rossi A, Merkus D, Klotz E, Mollet N, de Feyter PJ, Krestin GP. Stress myocardial perfusion: imaging with multidetector CT. *Radiology*. 2014;270(1):25–46. <https://doi.org/10.1148/radiol.13112739>.
- Danad I, Szymonifka J, Schulman-Marcus J, Min JK. Static and dynamic assessment of myocardial perfusion by computed tomography. *Eur Hear J – Cardiovasc Imaging*. 2016. <https://doi.org/10.1093/ehjci/jew044> jew044.
- Linde JJ, Sorgaard M, Kühl JT, et al. Prediction of clinical outcome by myocardial CT perfusion in patients with low-risk unstable angina pectoris. *Int J Cardiovasc Imaging*. 2017;33(2):261–270. <https://doi.org/10.1007/s10554-016-0994-x>.

23. Lu MT, Ferencik M, Roberts RS, et al. Noninvasive FFR derived from coronary CT angiography: management and outcomes in the PROMISE trial. *JACC Cardiovasc Imaging*. 2017;10(11):1350–1358. <https://doi.org/10.1016/j.jcmg.2016.11.024>.
24. Meinel FG, Pugliese F, Schoepf UJ, et al. Prognostic value of stress dynamic myocardial perfusion CT in a multicenter population with known or suspected coronary artery disease. *Am J Roentgenol*. 2017;208(4):761–769. <https://doi.org/10.2214/AJR.16.16186>.
25. Meinel FG, Ebersberger U, Schoepf UJ, et al. Global quantification of left ventricular myocardial perfusion at dynamic CT: feasibility in a multicenter patient population. *Am J Roentgenol*. 2014;203(2):174–180. <https://doi.org/10.2214/AJR.13.12328>.
26. Wichmann JL, Meinel FG, Schoepf UJ, et al. Absolute versus relative myocardial blood flow by dynamic CT myocardial perfusion imaging in patients with anatomic coronary artery disease. *Am J Roentgenol*. 2015;205(1):W67–W72. <https://doi.org/10.2214/AJR.14.14087>.
27. Tesche C, Cecco CN De, Baumann S, et al. Coronary CT angiography–derived fractional flow reserve: machine learning algorithm versus computational fluid dynamics modeling. *Radiology*. 0(0):171291. doi:10.1148/radiol.2018171291.
28. Farhad H, Dunet V, Bachelard K, Allenbach G, Kaufmann PA, Prior JO. Added prognostic value of myocardial blood flow quantitation in rubidium-82 positron emission tomography imaging. *Eur Heart J Cardiovasc Imaging*. 2013;14(12):1203–1210. <https://doi.org/10.1093/ehjci/jet068>.
29. Fukushima K, Javadi MS, Higuchi T, et al. Prediction of short-term cardiovascular events using quantification of global myocardial flow reserve in patients referred for clinical 82Rb PET perfusion imaging. *J Nucl Med*. 2011;52(5):726–732. <https://doi.org/10.2967/jnumed.110.081828>.
30. Ziadi MC, Dekemp RA, Williams KA, et al. Impaired myocardial flow reserve on rubidium-82 positron emission tomography imaging predicts adverse outcomes in patients assessed for myocardial ischemia. *J Am Coll Cardiol*. 2011;58(7):740–748. <https://doi.org/10.1016/j.jacc.2011.01.065>.
31. Yoshinaga K, Chow BJW, Williams K, et al. What is the prognostic value of myocardial perfusion imaging using rubidium-82 positron emission tomography? *J Am Coll Cardiol*. 2006;48(5):1029–1039. <https://doi.org/10.1016/j.jacc.2006.06.025>.
32. Dorbala S, Di Carli MF, Beanlands RS, et al. Prognostic value of stress myocardial perfusion positron emission tomography: results from a multicenter observational registry. *J Am Coll Cardiol*. 2013;61(2):176–184. <https://doi.org/10.1016/j.jacc.2012.09.043>.
33. Travin MI, Heller GV, Johnson LL, et al. The prognostic value of ECG-gated SPECT imaging in patients undergoing stress Tc-99m sestamibi myocardial perfusion imaging. *J Nucl Cardiol*. 2004;11(3):253–262. <https://doi.org/10.1016/j.nuclcard.2004.02.005>.
34. Shaw LJ, Iskandrian AE. Prognostic value of gated myocardial perfusion SPECT. *J Nucl Cardiol*. 2004;11(2):171–185. <https://doi.org/10.1016/j.nuclcard.2003.12.004>.
35. Pijls NHJ, van Schaardenburgh P, Manoharan G, et al. Percutaneous coronary intervention of functionally nonsignificant stenosis. 5-Year follow-up of the DEFER study. *J Am Coll Cardiol*. 2007;49(21):2105–2111. <https://doi.org/10.1016/j.jacc.2007.01.087>.
36. Pijls NHJ, de Bruyne B, Peels K, et al. Measurement of fractional flow reserve to assess the functional severity of coronary-artery stenoses. *N Engl J Med*. 1996;334(26):1703–1708. <https://doi.org/10.1056/NEJM199606273342604>.
37. De Bruyne B, Pijls NHJ, Kalesan B, et al. Fractional flow reserve–guided PCI versus medical therapy in stable coronary disease. *N Engl J Med*. 2012;367(11):991–1001. <https://doi.org/10.1056/NEJMoa1205361>.
38. Vliegthart R, De Cecco CN, Wichmann JL, et al. Dynamic CT myocardial perfusion imaging identifies early perfusion abnormalities in diabetes and hypertension: insights from a multicenter registry. *J Cardiovasc Comput Tomogr*. 2016;10(4):301–308. <https://doi.org/10.1016/j.jcct.2016.05.005>.
39. Crea F, Lanza GA, Camici PG. *Coronary Microvascular Dysfunction*. 2014; 2014. <https://doi.org/10.1007/978-88-470-5367-0>.
40. Crea F, Camici PG, Merz CNB. Coronary microvascular dysfunction: an update. *Eur Heart J*. 2014;35(17):1101–1111. <https://doi.org/10.1093/eurheartj/ehf513>.
41. Johnson NP, Kirkeeide RL, Gould KL. Is discordance of coronary flow reserve and fractional flow reserve due to methodology or clinically relevant coronary pathophysiology? *JACC Cardiovasc Imaging*. 2012;5(2):193–202. <https://doi.org/10.1016/j.jcmg.2011.09.020>.
42. Arena G, Morello A, D'Andrea A, et al. Relationship between fractional flow reserve (ffr) and coronary flow reserve (cfr) by pet in identifying coronary stenosis causing myocardial ischemia. *J Am Coll Cardiol*. 2017;69(11):133. [https://doi.org/10.1016/S0735-1097\(17\)33522-2](https://doi.org/10.1016/S0735-1097(17)33522-2).
43. Stillman AE, Oudkerk M, Bluemke DA, et al. Imaging the myocardial ischemic cascade. *Int J Cardiovasc Imaging*. 2018;0(0):0. <https://doi.org/10.1007/s10554-018-1330-4>.
44. Erthal F, Premaratne M, Yam Y, et al. Appropriate use criteria for cardiac computed tomography: does computed tomography have incremental value in all appropriate use criteria categories? *J Thorac Imag*. 2018;33(2):132–137. <https://doi.org/10.1097/RTI.0000000000000297>.
45. Johnson NP, Tóth GG, Lai D, et al. Prognostic value of fractional flow reserve: linking physiologic severity to clinical outcomes. *J Am Coll Cardiol*. 2014;64(16):1641–1654. <https://doi.org/10.1016/j.jacc.2014.07.973>.
46. Schelbert HR. FFR and coronary flow reserve: friends or foes? *JACC Cardiovasc Imaging*. 2012;5(2):203–206. <https://doi.org/10.1016/j.jcmg.2011.12.003>.
47. Adedj J, De Bruyne B, Floré V, et al. Significance of intermediate values of fractional flow reserve in patients with coronary artery disease. *Circulation*. 2016;133(5):502–508. <https://doi.org/10.1161/CIRCULATIONAHA.115.018747>.
48. Meinel FG, Wichmann JL, Schoepf UJ, et al. Global quantification of left ventricular myocardial perfusion at dynamic CT imaging: prognostic value. *J Cardiovasc Comput Tomogr*. 2017;11(1):16–24. <https://doi.org/10.1016/j.jcct.2016.12.003>.
49. Kim EY, Chung W-JJ, Sung YM, et al. Normal range and regional heterogeneity of myocardial perfusion in healthy human myocardium: assessment on dynamic perfusion CT using 128-slice dual-source CT. *Int J Cardiovasc Imaging*. 2014;30(1):33–40. <https://doi.org/10.1007/s10554-014-0432-x>.